



HAL
open science

Multi-omics analyses of sid2 mutant reflect the need of isochorismate synthase ICS1 to cope with sulfur limitation in *Arabidopsis thaliana*

Jie Luo, Marien Havé, Fabienne Soulay, Thierry Balliau, Gilles Clément, Frédérique Tellier, Michel Zivy, Jean-Christophe J.-C. Avice, Céline Masclaux-daubresse

► To cite this version:

Jie Luo, Marien Havé, Fabienne Soulay, Thierry Balliau, Gilles Clément, et al.. Multi-omics analyses of sid2 mutant reflect the need of isochorismate synthase ICS1 to cope with sulfur limitation in *Arabidopsis thaliana*. *The Plant Journal*, 2024, 118, pp.1635 - 1651. 10.1111/tpj.16702 . hal-04674667

HAL Id: hal-04674667

<https://hal.science/hal-04674667v1>

Submitted on 21 Aug 2024

HAL is a multi-disciplinary open access archive for the deposit and dissemination of scientific research documents, whether they are published or not. The documents may come from teaching and research institutions in France or abroad, or from public or private research centers.

L'archive ouverte pluridisciplinaire **HAL**, est destinée au dépôt et à la diffusion de documents scientifiques de niveau recherche, publiés ou non, émanant des établissements d'enseignement et de recherche français ou étrangers, des laboratoires publics ou privés.

Multi-omics analyses of *sid2* mutant reflect the need of isochorismate synthase ICS1 to cope with sulfur limitation in *Arabidopsis thaliana*

Jie Luo^{1,†,‡} , Marien Havé^{1,†,§} , Fabienne Soulay¹, Thierry Balliau² , Gilles Clément¹ , Frédérique Tellier¹, Michel Zivy² , Jean-Christophe Avicé³  and Céline Masclaux-Daubresse^{1,*} 

¹Université Paris-Saclay, INRAE, AgroParisTech, Institut Jean-Pierre Bourgin (IJPB), 78000 Versailles, France,

²UMR GQE- le Moulon, INRA, Université Paris-Sud, CNRS, AgroParisTech, Université Paris-Saclay, 91190 Gif-sur-Yvette, France,

³UMR 950 EVA (Ecophysiologie Végétale & Agronomie), INRAE, Normandie Université (UNICAEN), Federation of Research Normandie Végétal (Fed4277 NORVEGE), 14032 Caen, France

Received 27 October 2023; revised 7 February 2024; accepted 20 February 2024.

*For correspondence (e-mail celine.masclaux-daubresse@inrae.fr).

[†]These two authors contributed equally to this work.

[‡]Present address: College of Horticulture and Forestry Sciences, Hubei Engineering Technology Research Center for Forestry Information, Huazhong Agricultural University, Wuhan 430070, China

[§]Present address: Université Paris Est Créteil, CNRS, INRAE, IRD, Sorbonne Université, Université de Paris, Institut d'Ecologie et des Sciences de L'Environnement de Paris, IEES-Paris, F-94010, Créteil, France

SUMMARY

The *SID2* (SA INDUCTION-DEFICIENT2) gene that encodes ICS1 (isochorismate synthase), plays a central role in salicylic acid biosynthesis in *Arabidopsis*. The *sid2* and *NahG* (encoding a bacterial SA hydroxylase) overexpressing mutants (*NahG*-OE) have currently been shown to outperform wild type, presenting delayed leaf senescence, higher plant biomass and better seed yield. When grown under sulfate-limited conditions (low-S), *sid2* mutants exhibited early leaf yellowing compared to the *NahG*-OE, the *npr1* mutant affected in SA signaling pathway, and WT. This indicated that the hypersensitivity of *sid2* to sulfate limitation was independent of the canonical *npr1* SA-signaling pathway. Transcriptomic and proteomic analyses revealed that major changes occurred in *sid2* when cultivated under low-S, changes that were in good accordance with early senescence phenotype and showed the exacerbation of stress responses. The *sid2* mutants displayed a lower sulfate uptake capacity when cultivated under low-S and lower S concentrations in their rosettes. Higher glutathione concentrations in *sid2* rosettes under low-S were in good accordance with the higher abundance of proteins involved in glutathione and ascorbate redox metabolism. Amino acid and lipid metabolisms were also strongly modified in *sid2* under low-S. Depletion of total fatty acids in *sid2* under low-S was consistent with the fact that S-metabolism plays a central role in lipid synthesis. Altogether, our results show that functional ICS1 is important for plants to cope with S limiting conditions.

Keywords: salicylic acid, leaf senescence, sulfate metabolism, stress response.

INTRODUCTION

Salicylic acid (SA) is a phenolic plant hormone with important role in the systemic acquired resistance to pathogens and in the hypersensitive-reaction localized cell death (Dempsey & Klessig, 2017). SA plays also a role in plant response to a wide range of abiotic stresses. During plant development, SA is involved in the regulation of many senescence-related genes (Morris et al., 2000). Natural or synthesized analogues of SA are used as fungicides (Vergnes et al., 2014), for crop protection (Faize & Faize, 2018) or as biostimulants improve drought and salinity

tolerance (Hao et al., 2011; Khokon et al., 2011; Nazar et al., 2011). Few reports show that SA treatments facilitate mineral nutrient uptake and assimilation (Ghazizahani et al., 2014; Nazar et al., 2011).

In plant, the isochorismate synthase ICS1 (encoded by *SID2*, SA INDUCTION-DEFICIENT2) is required for SA synthesis (Wildermuth et al., 2001). The *sid2* mutants with no ICS1 activity, produce only 5–10% of the SA level observed in the wild type (WT). Another pathway involving the phenylalanine ammonia lyase (PAL) also contributes to SA synthesis but to a lower extent in *Arabidopsis* (Pokotylo

et al., 2019; Wu et al., 2022). Mutating *SID2* is not the only way to decrease SA level in plant. The *NahG* transgenic lines are also SA-deficient. These plants over-express the *NahG* gene from *Pseudomonas putida* strain G7 encoding bacterial salicylate hydroxylase that degrades SA (Mauch et al., 2001; You et al., 1991). Abreu and Munné-Bosch (2009) showed that the *sid2* mutant and the *NahG* transgenic line are both SA-deficient and present better growth rate, bigger rosettes, higher yield and that they maintain PSII photosystem capacity longer than the WT, thus suggesting that when grown under optimal growth conditions, the SA-deficient plants are more robust than WT. However, authors highlighted differences between *sid2* mutant and *NahG* transgenic line regarding the auxin IAA concentrations that were significantly higher in *sid2* seeds than in WT and *NahG*-OE plants.

Several reports show that SA can improve mineral use efficiency in plants by increasing sulfate and boron uptake, and nitrogen and sulfur assimilation (Ghazijahani et al., 2014; Nazar et al., 2011). Mineral use efficiency is very important for plant growth especially when fertilizers and/or nutrient availability in the soil are scarce. For many years, research in plant nutrition have focused efforts on nitrogen use efficiency, as large amounts of nitrate fertilizers are used worldwide and represent important costs for farmers and important issues for climate change (Havé et al., 2017). The decline of industrial sulfur dioxide (SO₂) emissions in the past decades is leading to the reduction of sulfate content in the soils (McNeill et al., 2005). This starts to have a negative impact on crop yield and seed quality (Dubousset et al., 2009) as well as some negative side-effects on nitrogen uptake (Dubousset et al., 2010; Gironde et al., 2014; Sorin et al., 2015). This is why several recent studies have paid more attention to the effect of sulfur limitation on plant physiology.

In this study, we examined the phenotypes of the *sid2* mutant when plants are cultivated under full nutrient or low sulfate (low-S) conditions. While we expected better performance of *sid2* mutant under low-S regarding the *sid2* phenotypes described in literature, we surprisingly observed early leaf yellowing in *sid2* in comparison to WT appearing on plants grown under chronic low sulfate nutrition. Transcriptomic, proteomic and metabolomic data revealed major differences between *sid2* mutant and WT plants under low sulfate. Altogether, our results show that functional ICS1 is important for plants to cope with S limiting conditions.

RESULTS

Arabidopsis *sid2* mutant displays early leaf yellowing phenotype when sulfate is limited

The *sid2* mutant and Col wild type (WT) were grown under short days in plethoric nitrate and sulfate condition (Ctrl),

under nitrate limitation (low-N), and under sulfate limiting condition (low-S). At 60 days after sowing (DAS), early leaf yellowing phenotypes were observed on the *sid2* plants under low-S condition by comparison to the WT (Figure 1; Figure S1). No difference between *sid2* and WT leaf yellowing was noticed under Ctrl conditions, and leaf yellowing was slightly delayed for *sid2* compared to WT under low-N condition (Figure S1). We then decided to focus on the low-S condition. Experiment was resumed using the SALK_042603 insertion line mutated in *SID2* (Sasek et al., 2014). The SALK_042603 plants recapitulated the early leaf yellowing phenotype observed on *sid2*, although phenotype was slightly less severe (Figure 2a,b). Like *sid2*, the SALK_042603 plants exhibited significantly lower chlorophyll concentrations in older leaves compared to WT (Figure 2c; Figure S2). Both *sid2* and SALK_042603 plants presented lower rosette biomass (mg dry weight (DW)) relative to WT under low-S (Figure 2d). The phenotypes of *NahG* over-expressing (*NahG*-OE) line and of *npr1* mutant were also examined. No early yellowing phenotype could be detected on either *NahG*-OE or *npr1* rosette leaves (Figure 1). Only reddish phenotype was observed on *NahG*-OE leaves, which was consistent with the higher anthocyanin concentrations in this line (Figure S2).

sid2 transcriptome under low-S condition reflects exacerbated stress responses

Transcriptome analyses were performed on rosettes of *sid2* and WT plants grown under low-S conditions for 60 days. Cutoff was made to keep genes showing fold changes (FC) >2 and FDR <0.05 between *sid2* versus WT under low-S (Dataset S1). We found 139 genes significantly differentially (DEGs) regulated in *sid2* vs. WT under low-S (99 up and 40 down regulated). The DEGs list was submitted to VirtualPlant1.3 BioMaps analysis to determine over-representation of terms using Fisher's exact test (with FDR correction), (Figure S3). Analysis revealed overrepresentation of oxidoreductase activity (GO:0016491) in the molecular functions, responses to biotic stimulus, stress, hydrogen peroxide and reactive oxygen species (GO:0050896; GO:0006950; GO:0070301; GO:0034614) in the biological process, and WRKY transcription factors (TF) in the Gene Family. *WRKY75* that accelerates leaf senescence in response to SA and oxidative stress was highly over-expressed in *sid2* (Guo et al., 2017), as well as *WRKY45*, which respond to phosphate starvation like *WRKY75* (Velasco et al., 2016). The decrease of the expression of the gene encoding the NIMIN-1 protein that interacts with NPR1 is a typical response to SA deficiency. Several DEGs genes are related to hormone signaling showing that in addition to SA, other hormonal responses as ethylene, abscisic acid, and gibberellin were also affected. It can be noticed that we did not find any strong effect of *sid2* on the transcript levels of JA-biosynthesis or



Figure 1. Leaf yellowing phenotype of *sid2* under low-S is different from *NahG* over-expressor, *npr1*, and WT. Plants were grown under control or low sulfate (low-S) conditions for 60 days after sowing.

JA-responding genes, except the up-regulation *JRG21* in *sid2* under low-S. (Thaler et al., 2012; Weigel et al., 2005). The differential expression of cytochrome P450 genes which are related to oxidative stress and camalexin biosynthesis reflects the exacerbation of stress-signaling in *sid2*. The GSEA representation (Figure S3) shows that the pathways involved in leaf senescence, plant organ senescence, response to decreased oxygen levels, response to hypoxia, and toxin metabolic process were activated in *sid2* vs. WT under low-S.

In order to determine whether *sid2* suffered from S limitation more than WT, we checked whether some low-S responding genes identified previously by Luo et al. (2020), were modified in the *sid2* transcriptome. Among the 40 genes downregulated in *sid2* relative to WT under low-S, 57% were assigned as low-S repressed genes in the study of Luo et al. (2020), as shown in dataset S1. Among the 99 genes up-regulated in *sid2* relative to WT under low-S, 78% were assigned as low-S downregulated genes by Luo et al. (2020). Therefore, a large proportion of the genes differentially expressed in *sid2* under low-S are genes responding to chronic S limitation. Comparing the transcriptome of *sid2* under low-S to the list of the SLIM1-dependent and SLIM1-independent sulfur responding genes published by Dietzen et al. (2020), we found that

among the DEGs, only 8 were qualified as SLIM1-independent sulfur responding genes and 1 as SLIM1-dependent S responding genes (Dataset S1).

We can notice that the genes usually used as marker for S starvation in literature like the *SULTR* sulfate transporters or *LSU* (response to low sulfur genes) were not in the DEGs list of low-S *sid2* (Sirko et al., 2015). This might be due to the fact that transcriptome was performed on leaves and not on roots.

Sulfate transporter genes are differentially expressed in the roots of *sid2* under low-S

The expression of sulfate transporters in the roots is a marker of S limitation. The expressions of *SULTR1.1*, *SULTR1.2*, *SULTR1.3*, and *SULTR2.1* were measured in the roots of WT and *sid2* plants grown under control or low-S conditions. All the *SULTR* genes were induced under low-S in both WT and *sid2* (Figure 3). Induction of *SULTR* genes by low-S was higher in *sid2* than in WT, except for *SULTR1.2*.

Proteome comparisons confirmed the hypersensitivity of *sid2* to low-S

Total proteins were extracted from the WT and *sid2* rosettes harvested 60 DAS, and submitted to shotgun LC–

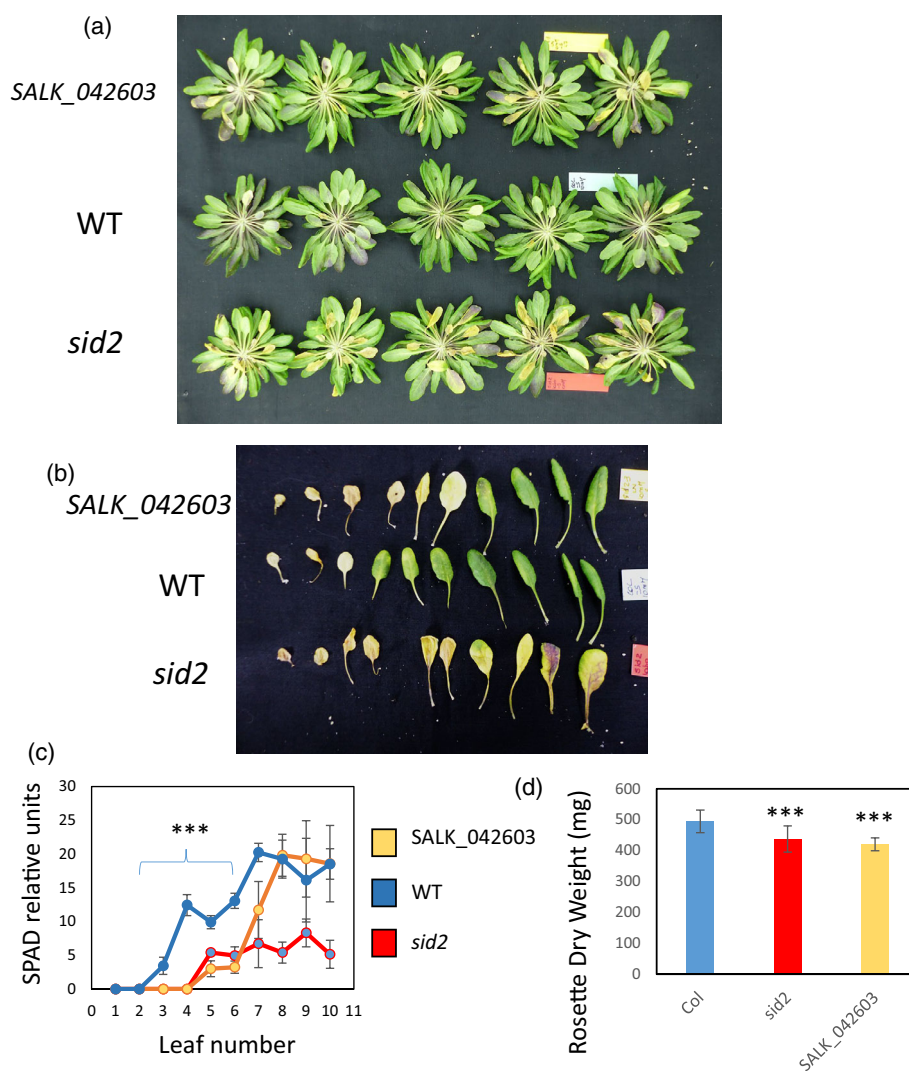


Figure 2. Both *sid2* and SALK_042603 SID2 mutants exhibit early leaf yellowing, lower chlorophyll concentration and lower biomass under low sulfur conditions.

Plants were grown under control or low sulfate (Low-S) conditions for 60 days after sowing. Early leaf senescence phenotypes can be observed on rosettes (a) and detached leaves (older and first emerged leaves on the left). Relative chlorophyll concentrations per cm² were determined on detached leaves using the DUALEX SCIENTIFIC+™ chlorophyll meter (ForceA, Orsay, France); (c; $n = 3$). The DW of the whole rosette was measured (d; $n = 9-10$). Leaf numbers increase from the oldest to the youngest. Mean and SD are shown. Statistical significance (T-test; $P < 0.001$) is indicated with ***.

MS–MS analyses according to Havé et al. (2018). Proteins were quantified by XIC (eXtracted Ion Chromatogram) and two kind of comparisons were performed: (i) low-S/Ctrl in *sid2* or WT, and (ii) *sid2*/WT under Ctrl or low-S conditions.

The first proteomic analysis revealed that there were 244 and 481 proteins significantly differentially accumulated under low-S (low-S DAPs) compared to control condition in WT and *sid2*, respectively (Dataset S2). These proteins were classified in different groups depending on their relative abundance in low-S versus Ctrl condition, in *sid2* or in WT (Figure 4a). Only 80 low-S DAPs were modified in both WT and *sid2*. They were modified in the same way by low-S in the two genotypes (61 up and 19 down;

Table S1; Figure 4a). For the down low-S DAPs, Virtual-Plant1.3 BioMaps analysis using Fisher Exact Test (with FDR correction) revealed overrepresentation of sulfate adenylyltransferase activity (GO:0004779) in the molecular function assignments by TAIR, and of inorganic nutrient metabolism by AraCyc Pathways. For the 61 up low-S DAPs, overrepresentation of proteins related stress response, oxylipin synthesis, jasmonic acid synthesis, fatty acid metabolism, IAA-amino acid conjugates, and plant hormones was revealed (Table S1).

The second proteome analysis identified the proteins significantly (FDR < 0.05) differentially accumulated in *sid2* compared to WT (*sid2* DAPs) under Ctrl or low-S conditions (Dataset S3). Among the 473 *sid2* DAPs, 467 were exclusively

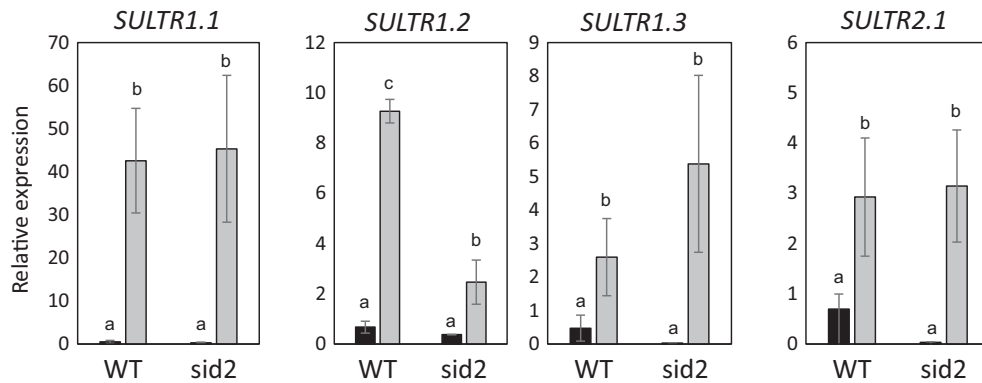


Figure 3. Expression of *SULTR* genes under low-S in roots of *sid2* and WT. Roots were collected 15 days after sowing from WT (Col) and *sid2* seedlings grown on vertical plates under control (Ctrl; black bars) or low sulfate (low-S; gray bars) conditions. Expression levels of genes were normalized to the geometrical mean of the three reference genes (*UBC21*, *Actin 2* and *EF1 α*). Bars indicate mean \pm SD ($n = 3$). Different letters above bars indicate statistically significant differences (P -value < 0.05).

modified under low-S and 5 exclusively under Ctrl condition (Dataset S3). This showed that under sufficient sulfate condition the proteomes of *sid2* and WT are not different, while substantial changes are induced under low-S. Among the 473 *sid2* DAPs, 192 were less abundant in *sid2* and 275 more abundant in *sid2* than in WT. The VirtualPlant 1.3 analysis (with FDR correction) of the 192 DAPs depleted in *sid2* under low-S revealed significant overrepresentation of terms related to ribosome and translation, water deprivation and aquaporins, C1 compounds, tetrapyrrole, CO₂ fixation and Calvin/Benson cycle. The examination of the 275 up-accumulated *sid2* DAPs revealed enrichment in GO terms related to stresses, polymer degradation, glycoside hydrolases, energy and amino acid metabolisms (Table S2). The Mapman metabolism overview presented in Figure 5a illustrates the higher contents of proteins related to the ascorbate/glutathione metabolisms, and the strong depletion of proteins involved in the Calvin/Benson cycle and the light-dependent reactions of the photosynthesis. Overview of the proteins related to abiotic stress represented in Figure 5b reflects the strong modifications related to the redox state and the overaccumulation of glutathione-S-transferases, the increases of proteins related to proteolysis, cell wall degradation and auxin metabolism. The overrepresentation of translation related proteins in the down *sid2* DAPs (Figure S4) was in good agreement with the decrease in the abundance of cytosolic and plastid ribosomal proteins and plastid tRNA ligases (Figure S3). The suggested depletion of ribosomes in *sid2* under low-S was consistent with the lower abundance of rRNA measured in *sid2* under low-S condition (Figure 6).

Predicted protein–protein interaction networks

To construct the protein–protein network, the known and predicted protein–protein associations were analyzed using the STRING database (<https://string-db.org/>). With the high confidence scores 0.9, a total of 205 DAPs, identified in *sid2* vs. WT under low-S condition, shared 699 potential

interactions (Figure 7). The predicted protein–protein network revealed the major biological changes in *sid2* vs. WT under low-S. Several DAPs involved in major CHO metabolism and in protein folding and degradation were significantly up-accumulated in *sid2*. DAPs participating in protein synthesis, tetrapyrrole synthesis and vesicle transport were less-accumulated *sid2*. Interaction network emphasized a decrease in photosynthetic activity in *sid2* under low-S and the decrease of protein synthesis that was paralleled by exacerbated protein degradation. The vesicle transport hub was mainly related to proteins involved in clathrin coated vesicles budding and trafficking.

Sulfur-related metabolism is modified in *sid2* when sulfate supply is limited

Comparison of the proteomes reveals no remarkable changes for sulfur-related enzymes, transporters or regulators (Figure 8; Table S3). Nevertheless, the total sulfur concentration in the rosettes of *sid2* plants was sharply lower than in WT when cultivated under Low-S (0.1% versus 0.16%; Figure 8 inset a) and under control condition (Figure 8 inset b). The lower S concentrations in the rosettes of *sid2* and the lower expression levels of *SULTR1; 2* in *sid2* roots (Figure 3) suggest that sulfate uptake was impaired in *sid2* plants. Few enzymes involved downstream of sulfate reduction as the STR2 thiosulfate:cyanide sulfurtransferase were more abundant in *sid2* than in WT (Figure 8). The higher abundance of several superoxide dismutases (SOD) and of several dehydroascorbate reductases (DHAR) reflected the hypersensitivity of *sid2* to low-S. The stimulation of the ascorbate/glutathione pathways and the higher glutathione concentration in *sid2* (Figure 8 inset c) reflected that sulfur metabolism was dedicated to the control of redox homeostasis. The higher contents in the SOT17 and SOT16 enzymes in *sid2* under Low-S suggests that glucosinolate metabolism was also stimulated.

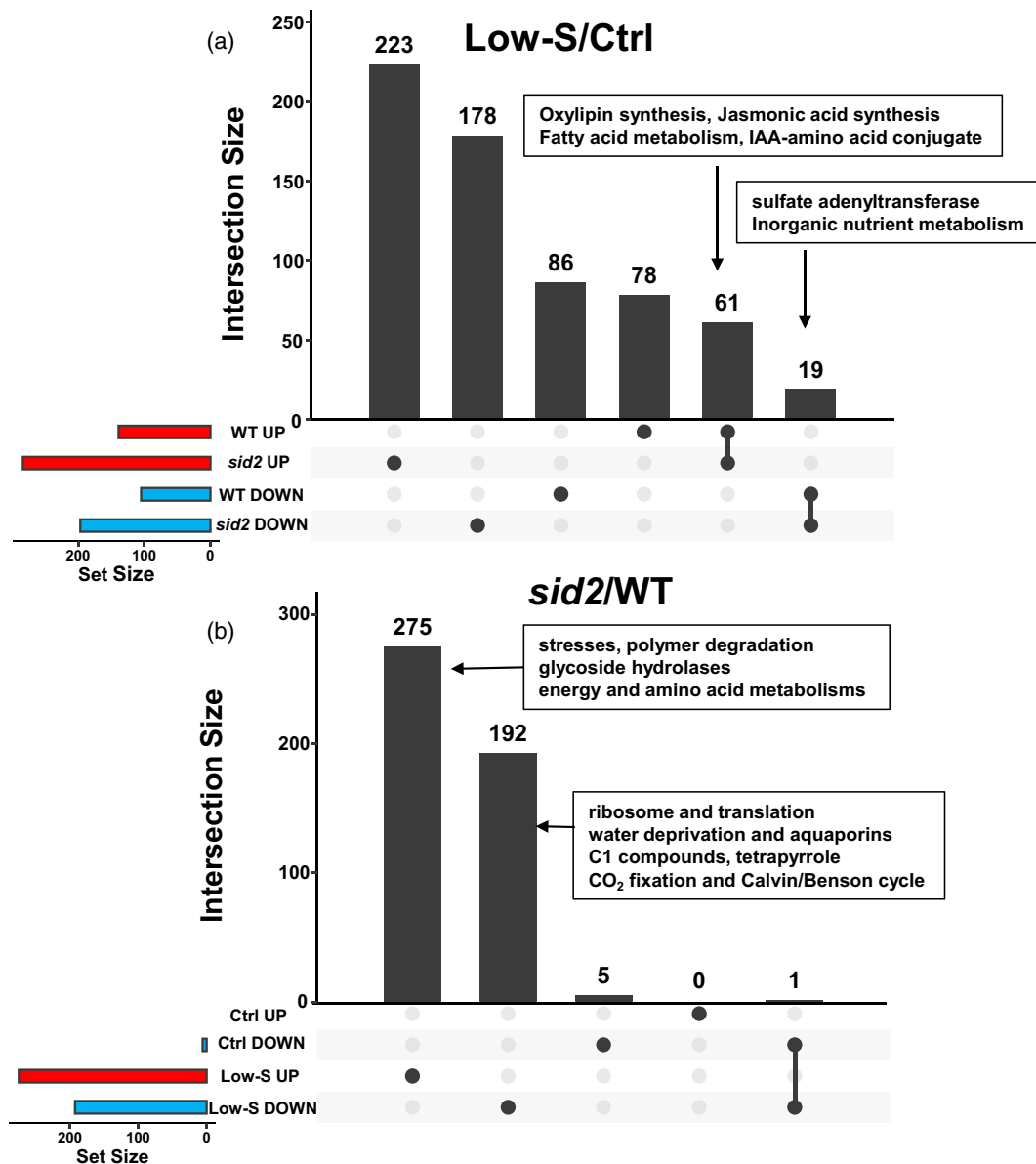


Figure 4. Upset plot for overlapping up- (in red) or down (in blue) DAPs in (a) low-S compared to control (Ctrl) condition in *sid2* or WT, and in (b) *sid2* relative to WT under control (Ctrl) or low-S conditions.

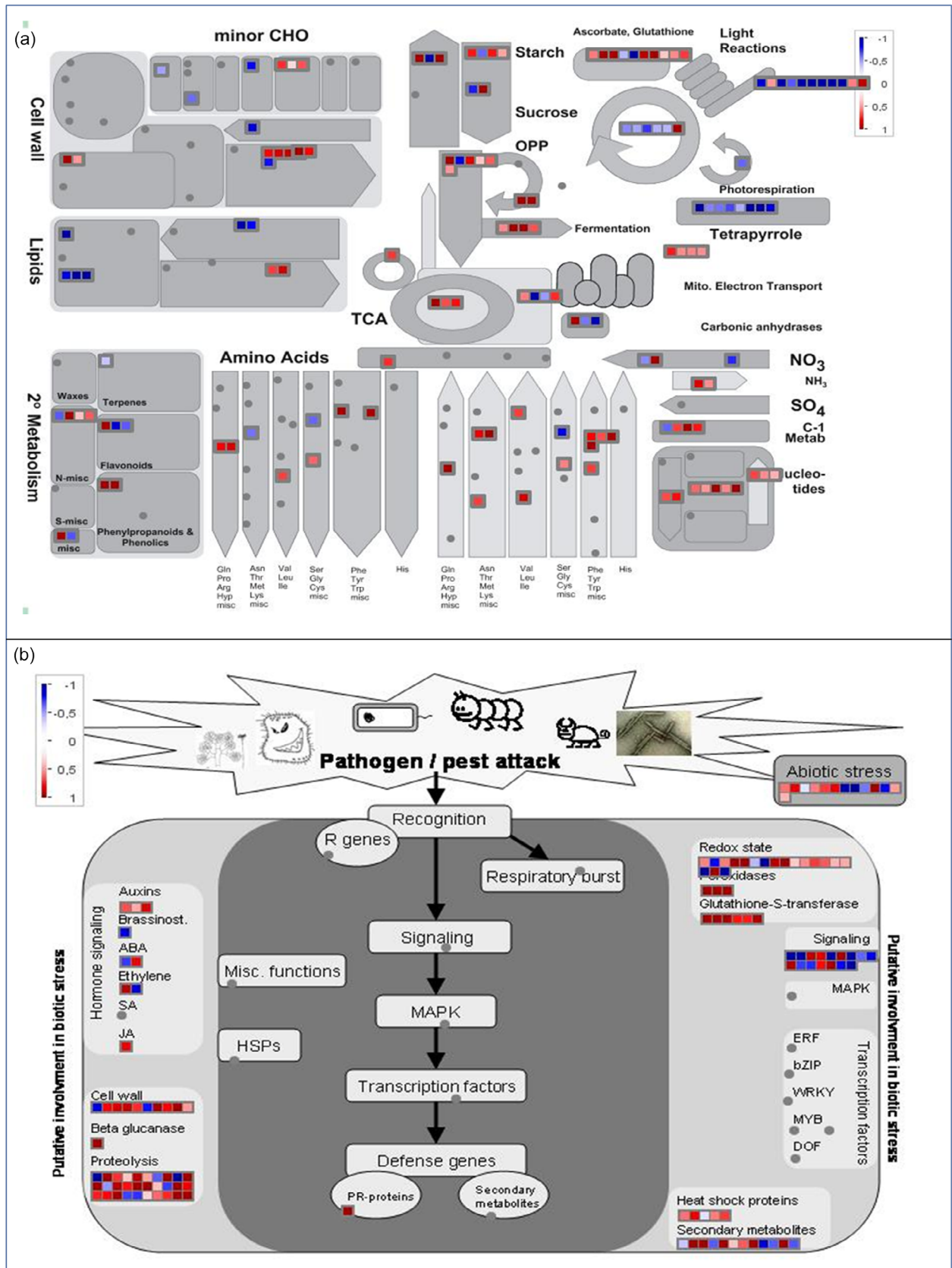
The number of genes in each category is indicated on top of each bar. Statistically significant functional categories overrepresented in the set of DAPs Up or Down accumulated in both conditions (a) or both genotypes (b) are indicated in the insets.

S uptake is lower when *SID2* is mutated

In order to determine whether mutation in *SID2* affects S-uptake, the *sid2* and SALK_042603 lines were cultivated under low-S condition for 60 days, then labeled for 24 h with ³⁴S nutritive solution. Measurement of ³⁴S abundance

in root and shoot 24 h post-labelling permitted to estimate S-uptake at root and shoot levels. While there was no difference for ³⁴S concentration in the shoot between WT and mutants (Figure 9b), the lower biomass of mutant shoots (Figure 9a) resulted in lower ³⁴S content in the shoots of

Figure 5. Overview of the major proteomic changes occurring in the metabolic pathways and abiotic stress response in *sid2* by comparison to WT under low-S. Schematic representations of changes occurring in *sid2* under low sulfate condition were obtained from MapMan software (<https://mapman.gabipd.org/>). Over-accumulations in *sid2* are represented in red, and depletion in *sid2* are represented in blue according to the scale bars that represent the log₂ of fold changes of significant DAPs.



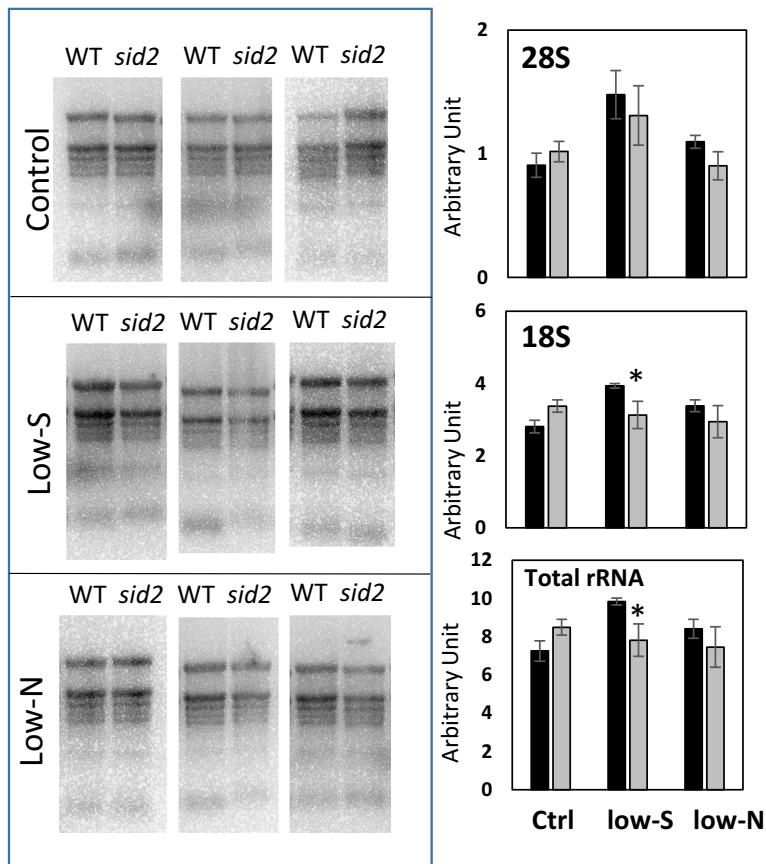


Figure 6. Significant changes in the abundance of rRNA in *sid2* are consistent with depletion of ribosomal and translation machinery proteins. Total RNAs were extracted from rosette leaves of *sid2* (gray bars) and WT (black bars) plants grown under low-S, low-N and control conditions for 60 DAS as shown in Figure S1. The extract volumes loaded in each lane were normalized on the basis of equal fresh weight. RNAs were revealed using ethidium bromide. Quantification of bands using ImageJ are presented in histograms for each condition ($n = 3$, t -test, * $P < 0.05$).

the two *SID2* defective mutants (Figure 9c). Biomass of *sid2* root was significantly lower than that of mutant. The root biomass of the SALK_042603 line also tended to be lower than WT root biomass, but this was not significant. Nevertheless, both ^{34}S concentrations and ^{34}S contents were lower in the roots of *sid2* and SALK_042603 compared to WT, showing that ^{34}S root uptake was affected in the *SID2* deficient plants.

Changes in amino acid and lipid contents in *sid2* are specific of the low-S condition

Metabolite profiling was performed using GC-MS to analyze changes in metabolites and S-amino acids in *sid2* relative to WT under low-S (Figure 10; Dataset S4). GC-MS analysis confirmed that salicylate and glycosylsalicylate were significantly less abundant in *sid2* than in WT. Strikingly, almost all the amino acids, including GABA and methionine, ethanolamine, putrescine, several sugars and TCA metabolites (aconitate, citrate, 2-oxoglutarate) related to amino acid metabolism, were over-abundant in *sid2* specifically under low-S. Accumulations of ascorbate, dehydroascorbate and tocopherols showed the higher abundance of antioxidant molecules in *sid2* under low-S.

Sulfur is essential for lipid metabolism in plant. As proteome comparisons detected higher abundance in

several proteins involved in lipid metabolism, we monitored total fatty acid concentrations using the FAMES method. Consistent with the sulfur depletion of *sid2* under low-S, total fatty acid concentrations were lower in *sid2* relative to WT, especially under low-S condition (Figure 11). The sulfoquinovosyldiglyceride (SQDG) are plant specific chloroplast galactolipids that contain sulfur. We were unfortunately not able to measure SQDG, but we postulated that a deficit in SQDG would be compensated by a higher amount in the other MGDG/DGDG galactolipids from chloroplast membranes. Interestingly, both MGDG and DGDG were significantly more abundant in *sid2* relative to WT, and this exclusively under low-S (Figure 11e,f).

DISCUSSION

The early leaf yellowing phenotype observed on *sid2* compared to WT under sulfate limitation prompted us to analyze the transcriptome, proteome and metabolome of the *sid2* and WT rosettes from plants grown under chronic sulfate limitation. Transcriptomic data revealed only few DEGs in *sid2* under Low-S. These DEGs reflected the higher expression of several senescence-associated WRKY transcription factors and of many stress related genes (Kim et al., 2018). Only few genes related to sulfur metabolism were differentially expressed in *sid2* relative to WT under

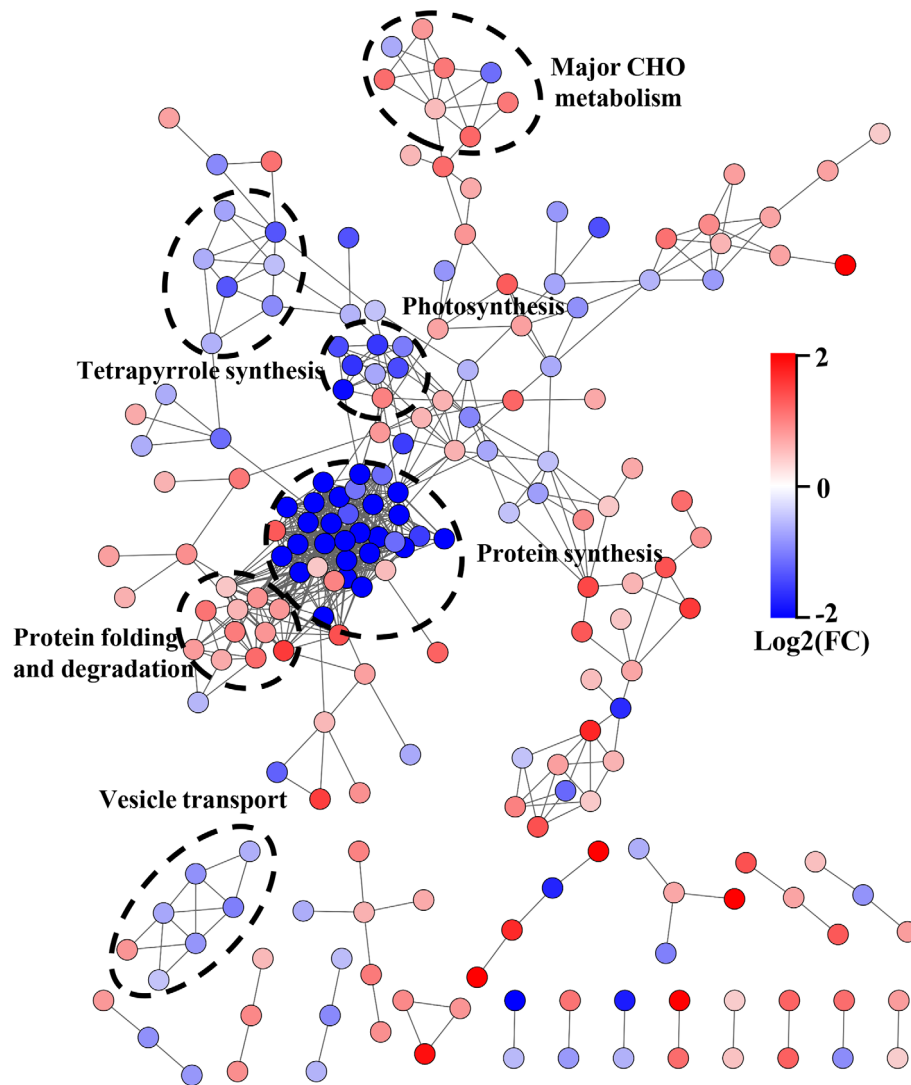
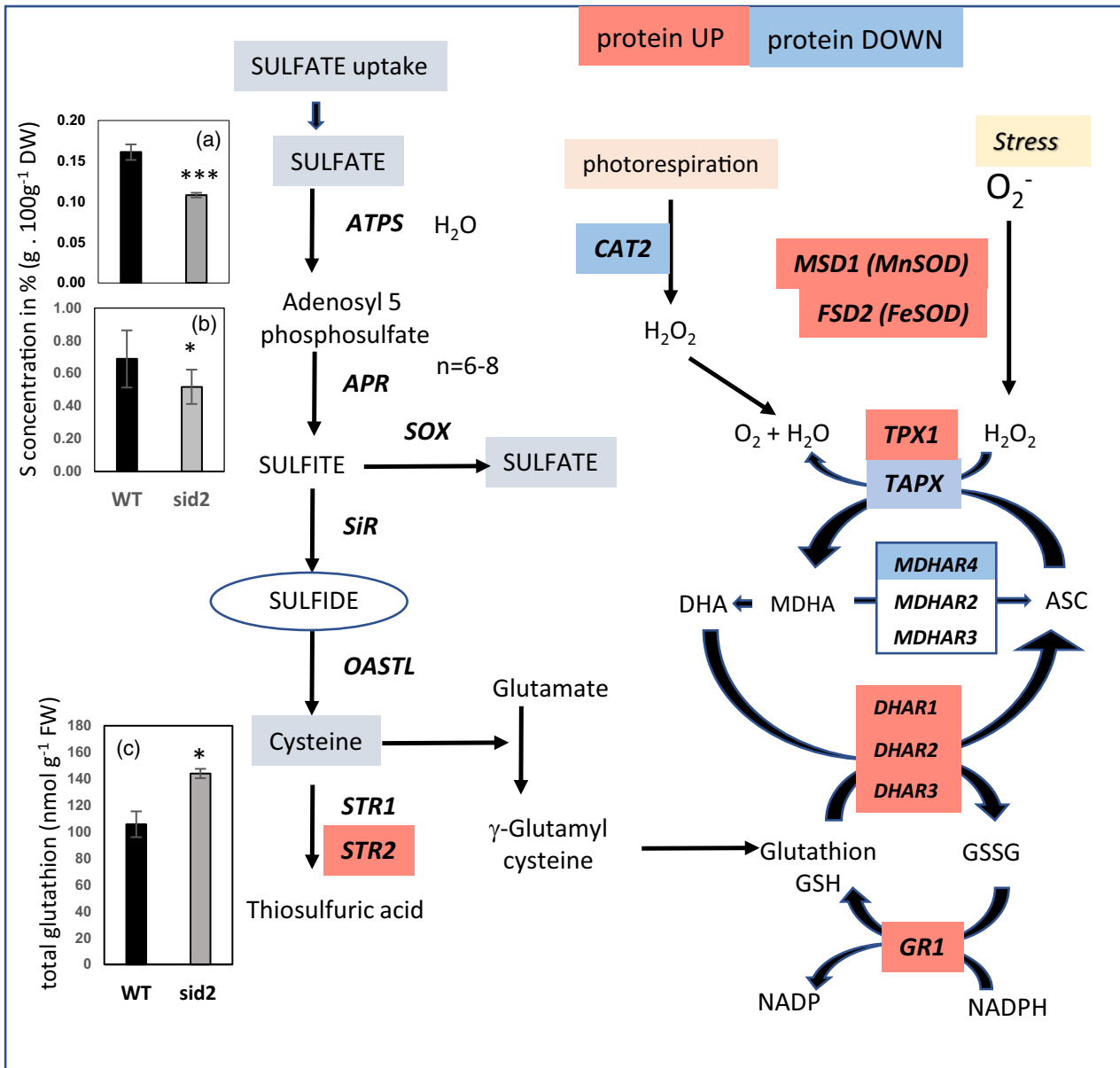


Figure 7. The predicted protein–protein association network of the DAPs identified in *sid2* vs wild type under low-S condition. The networks were constructed according to the results obtained from STRING database (<http://string-db.org/>) with confidence scores above 0.9. The network was visualized in Cytoscape software (version 3.8.2). Red and blue colors indicate DAPs with respectively higher and lower abundances in *sid2* under control or low-S condition compared to the wild type.

low-S. These genes are mostly related to the glutathione metabolism. A large proportion of the 139 DEGs correspond to genes previously identified by Luo et al. (2020) as responding to low-S. One of them was qualified as a SLIM1-regulated gene according to Dietzen et al. (2020) and eight of them correspond to genes regulated independently of SLIM1. SLIM1 was not found in the *sid2* DEGs. Thus, assumption of an interaction between SID2 and the SLIM1 central regulator in the control of these sulfur responsive gene is weak. Response to sulfur is certainly dependent on other regulators in *sid2*.

While the proteomes of *sid2* and WT did not differ much from each other under control condition (less than 10 DAPs under Ctrl), the number of DAPs in *sid2* greatly

increased when plants were grown under low sulfate condition. The lower abundance of proteins involved in translation, photosynthesis light chain reactions, tetrapyrrole synthesis, CO₂ fixation and response to water deprivation, and the higher abundance of proteins related to stress, carbohydrate degradation and lipid and amino acid metabolisms, emphasized the higher susceptibility of *sid2* plants to low-S and suggested major changes in metabolite contents. Metabolite profiling using GC–MS confirmed modifications in amino acid and sugars concentrations in *sid2* specifically under low-S. Lipid quantification using LC–MS revealed a depletion of fatty acids in *sid2* under low-S. Enzymatic and elemental measurements revealed respectively the over-accumulation of glutathione and the



depletion of sulfur in *sid2* under low-S. All these changes and especially those in glutathione, lipid and S concentrations, suggested that S fluxes from uptake to assimilation were altered in the *sid2* mutants under sulfate limitation, and that allocation in the different metabolic pathways was unbalanced. Modification in lipid composition and overaccumulation of MGDG and DGDG indeed suggested that the

chloroplast SQDG sulfolipids did not benefit from enough sulfur to be synthesized (Dibble et al., 2022). The lower total S concentration in *sid2* and the over-accumulation of glutathione, suggested that S was lacking for other metabolic pathways and possibly for protein synthesis. The lower abundance of many ribosomal proteins, t-RNA ligases, and rRNAs reflected accordingly lower translation

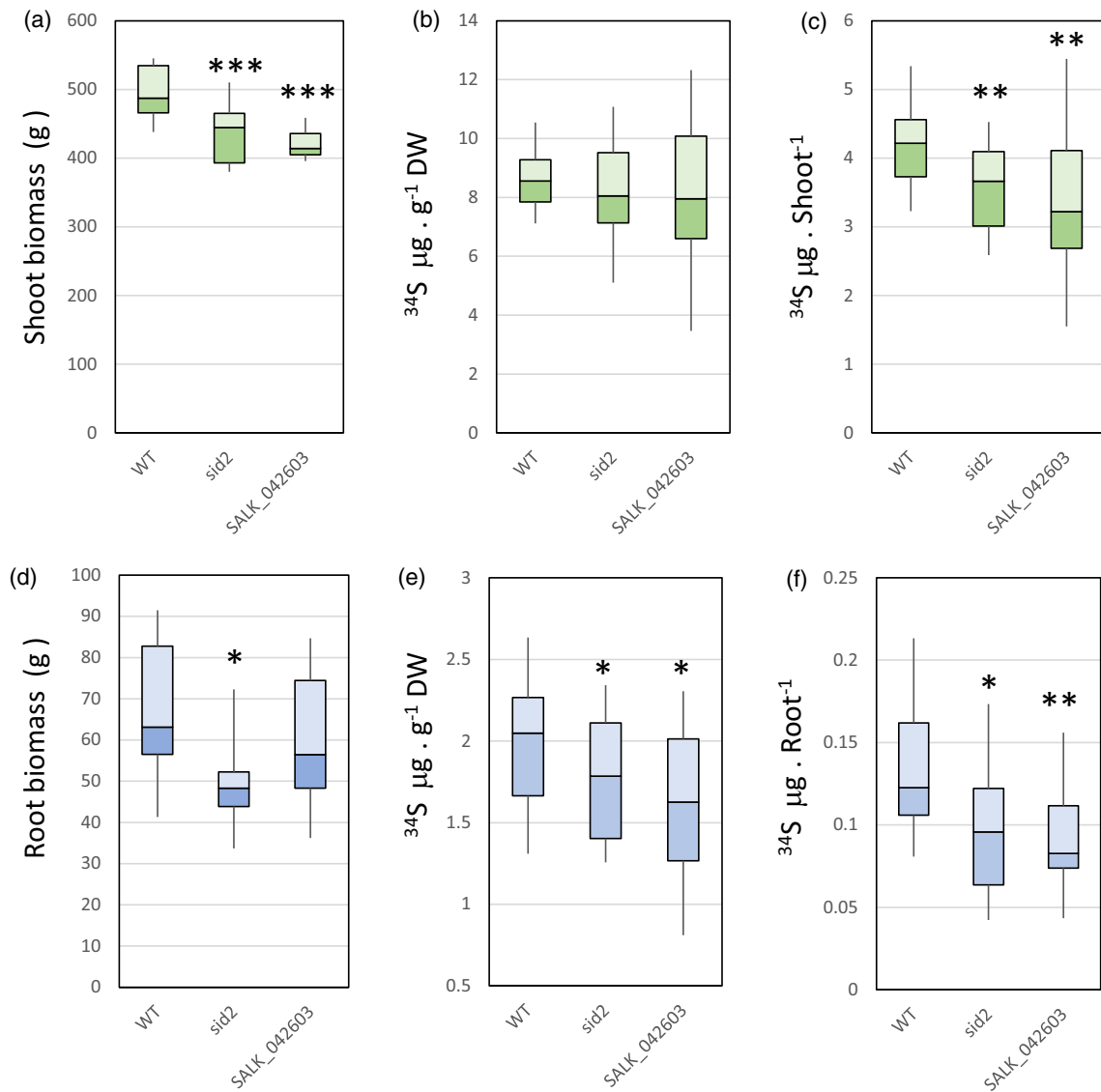


Figure 9. Sulfate uptake is lower in *SID2* deficient mutants compared to WT. ^{34}S labelling was performed over 24 h on plants cultivated under low-S for 60 days. At the end of the labelling period, ^{34}S enrichment was determined using IRMS. Biomass of shoot (a) and root (b) were determined measuring fresh weights. ^{34}S concentrations and ^{34}S contents in shoot (b, c) and root (e, f) were calculated from IRMS measurements. Box plot representation was performed from results obtained on $n = 8\text{--}9$ plant repeats. Statistically significant differences between WT and mutants are indicated with asterisks (t -test, * $P < 0.05$; ** $P < 0.01$; and *** $P < 0.001$).

activity in *sid2* under low-S. Whether lower translation in *sid2* was a result of premature senescence or a response to unbalanced sulfur allocation in metabolic pathways, remains to be determined. As Speiser et al. (2018) showed that a decrease of the metabolic flux from cysteine to glutathione, promotes the reallocation of cysteine and methionine towards protein translation by increasing ribosome abundance, we may suspect that low sulfate uptake and exacerbated glutathione synthesis had a negative effect on translation activity.

The lower concentration of sulfur in *sid2* rosettes and the higher expression of several high-affinity sulfate

transporters in *sid2* roots (Abdallah et al., 2010; Gironde et al., 2014; Rouached et al., 2008) was a sign of sulfate limitation. The $^{34}\text{SO}_4^{2-}$ labelling experiment confirmed that sulfate uptake was lower in the *sid2* and SALK_042603 mutants compared to WT under low-S condition. A defect of sulfate uptake in *sid2* plants can explain their hypersensitivity to sulfate limitation.

The question of the role of SA in this story remains open. Few publications report the positive effect of SA application on sulfate uptake (Ghazijahani et al., 2014; Nazar et al., 2011), and we can suspect that the defects of *sid2* mutant at sulfate absorption is linked to SA

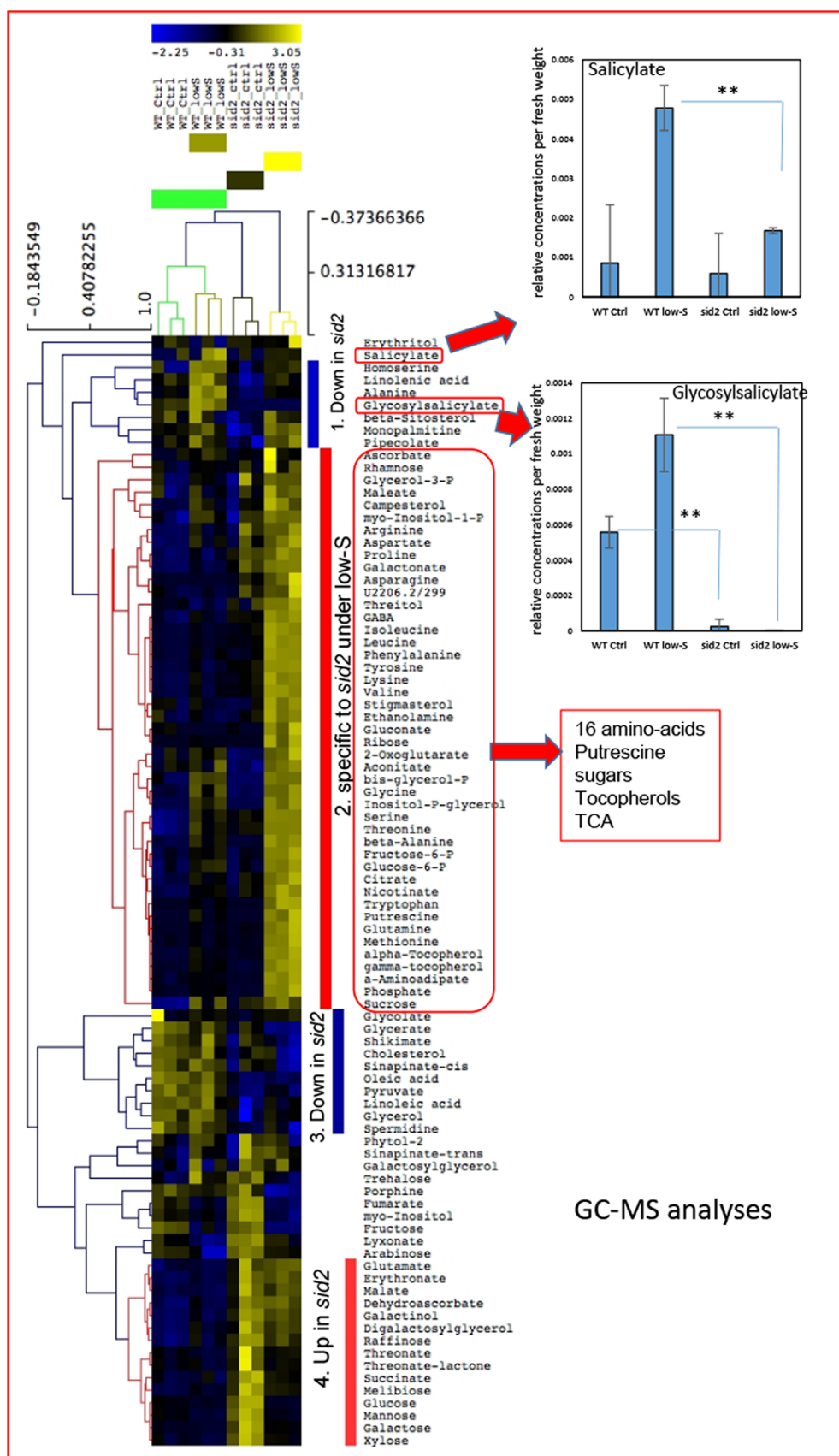
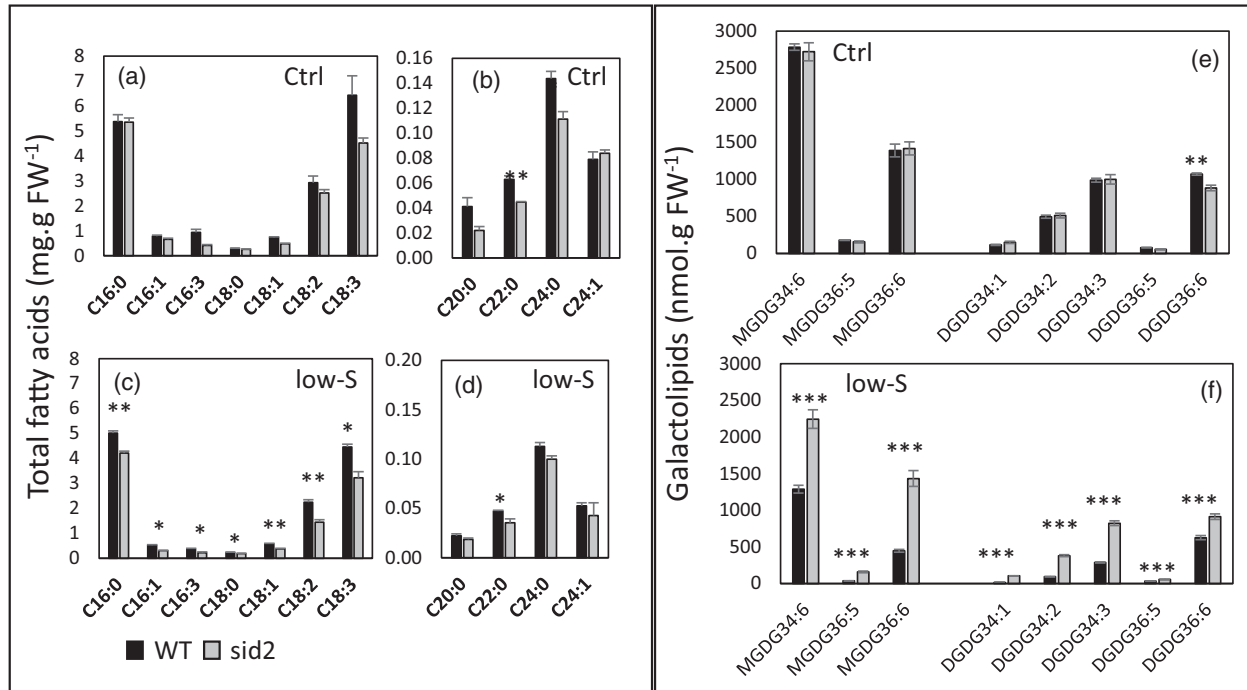


Figure 10. Hierarchic clustering of metabolite relative contents in *sid2* and WT under control and low-S conditions.

Metabolites were extracted from rosettes of *sid2* and Col-0 wild type plants grown under control and low sulfate conditions for 60 days. Quantification of metabolite concentrations was performed using GC-MS. Only significantly different metabolites, identified using ANOVA, are shown ($n = 3$). The hierarchic clustering was performed using MEV4. Metabolites specifically modified in *sid2* under low-S are grouped in the red shape. Salicylate and glycosylsalicylate relative concentrations are shown in histograms. Statistically significant differences are presented according to *t*-tests (** $P < 0.01$).

**Figure 11.** Concentrations of total fatty acids and galactolipids are different in *sid2* mutant under low-S.

Total fatty acids (a–d) and galactolipids (e, f) were measured in rosettes of Col-0 wild type (black bars) and *sid2* (gray bars) plants grown under control (a, b, e) and low sulfate (c, d, f) conditions for 60 days. Quantification of total fatty acids concentrations was performed using LC-MS. The mean and standard deviation are presented. Statistically significant differences were determined using *t*-tests ($n = 3$, ** $P < 0.01$).

production and possibly SA root exudation (Figure 12). However, the fact that the NahG-OE do not display any senescence phenotype suggests that *sid2* hypersensitivity to low-S is SA-independent. The absence of phenotype for the *npr1* mutant under low-S suggests that the *sid2* phenotype is independent of SA signaling. While SID2 (ICS1) plays a prominent role in SA synthesis (Wildermuth et al., 2001), *sid2* mutation significantly alters other hormone pathways. It was shown in Arabidopsis that *sid2* mutation increases ABA and ethylene concentrations in Arabidopsis (Abreu & Munné-Bosch, 2009). Our transcriptomic and proteomic data show indeed several auxin responsive genes/proteins differentially expressed/accumulated in *sid2* compared to WT under low-S. Could the hypersensitivity of *sid2* to S limitation be due to hormones other than SA? It is known that the degradation of SA by the NahG bacterial salicylate hydroxylase releases catechol, which are potent iron chelators (Peng et al., 2021). Does catechol production in the NahG overexpressor

(Shen et al., 2016) mitigate the effects of sulfur deficiency by restoring the S/Fe balance and FeS protein contents?

In conclusion, our study provides several lines of evidence that sulfate uptake and metabolism are impaired in *sid2* mutants (Figure 12). While sulfate uptake and assimilation are probably a bottleneck in the development of *sid2* plants under low-S, the high activity of antioxidant metabolism linked to glutathione synthesis can create major disorders by unbalancing sulfur fluxes dedicated to different metabolic pathways, and in particular to protein translation activity.

MATERIALS AND METHODS

Plant material and growth conditions

The *Arabidopsis thaliana* (L.) *sid2* mutant (Wildermuth et al., 2001), that has a single nucleotide substitution C to T in exon 9 leading to the conversion Glu449STOP, the NahG over-expressing line and the *npr1* mutant were kindly provided by Dr K. Yoshimoto

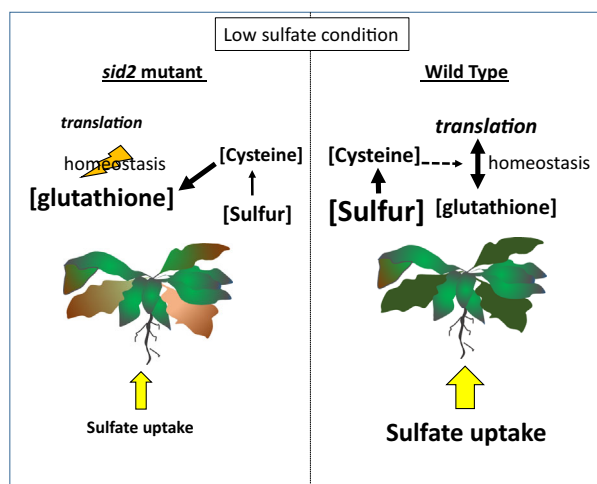


Figure 12. Schematic representation of the different responses of *sid2* mutants and wild type plants to low sulfate availability.

The size of the characters indicates the relative abundance of elements, metabolite and proteins involved in the processes of sulfate assimilation in *sid2* compared to wild type. Yellow arrows represent the sulfate uptake.

(Meiji University, Japan). These mutants have been widely studied and used in combination to other mutants to mitigate SA effects. The SALK_042603 line was kindly provided by Dr Eric Ruelland (CNRS, Université Paris Créteil, France).

Plants were cultivated in growth chambers according to Havé et al. (2018), under control conditions (Ctrl; 10 mM NO_3^- and 0.266 mM SO_4^{2-}), low nitrate (low-N; 2 mM NO_3^- and 0.266 mM SO_4^{2-}) or low sulfate (low-S; 10 mM NO_3^- and 0.016 mM SO_4^{2-}) conditions using the watering solutions described in the Table S4. For control and low-S conditions, each pot contained one plant; under low-N conditions there was six plants per pot. Whole rosettes were harvested 60 DAS. Four independent plant replicates were obtained. For control and low-S conditions, each biological replicate contained 4 rosettes. For low-N conditions, biological replicates contained 24 rosettes each. Harvests were performed between 10:00 and 11:00 AM, and samples were stored at -80°C for further experiments. Plant culture was repeated 3 times, providing samples from 3 independent experiments.

Vertical plates used to grow WT and *sid2* plantlets for root harvest contained different sulfate concentrations as indicated in Table S5.

Plant phenotyping

The variation of phenotyping in response to low-S and N conditions was monitored by the determination of chlorophyll, anthocyanin and flavonoid index using the DUALEX SCIENTIFIC+™ (ForceA, Orsay, France) fluorimeter.

Shotgun proteomic analysis

Leaf total proteins extraction, trypsin digestion, LC-MS/MS analysis and protein identification were performed according to Havé et al., 2018 (see the Supplementary information) at the PAPSSO platform (INRA, Le Moulon, Gif sur Yvette). For each sample, 40 μg of proteins were digested and the resulting peptides were analyzed by LC-MS/MS. Peptide quantification by peak area

integration on eXtracted ion chromatogram (XICs) was performed using the MassChroQ software (pappso.inra.fr/bioinfo/masschroq/). Normalization was performed considering peptide retention time. Proteins were then quantified based on peptide intensities by filtering for protein-specific peptides present in at least 90% of the samples and showing a statistically significant correlation ($r > 0.6$) with the other peptides of the same protein. Relative protein abundances were then calculated and defined as the sum of XICs intensities of selected peptides. When the peptides of a protein were not present or not reproducibly observed in one or several conditions, spectral counting (SC) was used in place of XICs analysis. Only proteins that produced at least four protein-specific spectra in at least one sample were considered for SC quantification. We considered that proteins which did not match this threshold were of too low abundance to be reliably quantified. The mass spectrometry proteomics data have been deposited to the ProteomeXchange Consortium via the PRIDE (<https://www.ebi.ac.uk/pride/pride>) partner repository with the dataset identifier PXD029638 and are provided as Dataset S5.

Transcriptome analyses and data mining

Total RNAs were extracted from rosettes leaves using Trisol[®] according to manufacturer's instructions. Biotinylated cRNA targets were prepared from 200 ng of total RNAs using the "MessageAmp[™] Premier RNA Amplification Kit" from Ambion, according to the Instruction Manual (#4386269 Revision B, 18 september 2007). Following fragmentation, 10 μg of cRNAs were hybridized for 16 h at 45°C , 60 rpm on GeneChip[®] Arabidopsis ATH1 Genome arrays (Affymetrix, at the Plateforme Biopuces et Séquençage of IGBMC, Strasbourg, France) interrogating over 24 000 genes. The chips were washed and stained in the GeneChip[®] Fluidics Station 450 (Affymetrix) using the FS450_0004 script and scanned with the GeneChip[®] Scanner 3000 7G (Affymetrix) at a resolution of 2.5 μm . Raw data (CEL Intensity files) were extracted from the scanned images using the Affymetrix GeneChip[®] Command Console (AGCC) version 4.0. The transcriptomic data have been deposited in NCBI's Gene Expression Omnibus (Edgar et al., 2002) and are accessible through GEO Series accession number GSE185514 (<https://www.ncbi.nlm.nih.gov/geo/query/acc.cgi?acc=GSE185514>) and are provided as Dataset S6.

Construction of the protein-protein interaction network

The DAPs identified under low-S condition compared to control condition in *sid2* mutant were submitted to STRING database (<http://string-db.org/>) (Szklarczyk et al., 2021) to construct the protein-protein interaction network with the confidence scores above 0.9. The results of the network were visualized in Cytoscape software (version 3.8.2) (Shannon et al., 2003).

Uptake measurement after ^{34}S labelling

At 60 days after sowing, plants grown on sand were labeled for 24 h using a labeled control solution containing ^{34}S isotopes (2.5% enrichment). At the end of the 24 h labelling period rosettes were cut from the root and harvested. Then roots were separated from sand, briefly rinsed with distilled water, and collected. Both shoot and root matter were dried. The DW of root and shoot was measured. Then the ^{34}S concentrations were determined using IRMS as described in Lornac et al. (2020). Relative concentration of sulfur was measured on dry matter using elemental analyzer EA3000 (Eurovector, Mila, Italy) according to (Dubouset et al., 2010).

Metabolite and lipid extractions and analyses

Total fatty acids, originating from all the lipids present in the cell, and galactolipids were measured according to Havé et al. (2019).

For metabolite profiling using GC–MS, extraction, derivatization, analysis, and data processing were performed according to Clément et al. (2018). Raw Agilent datafiles were converted in NetCDF format and analyzed with AMDIS (<http://chemdata.nist.gov/mass-spc/amdis/>). A home retention index mass spectra library built from the NIST, Golm, and Fiehn databases and standard compounds was used for metabolite identification. Peak areas were then determined using the quanlynx software (Waters) after conversion of the NetCDF file to masslynx format. Metabolites were annotated and their levels on a fresh weight basis were normalized with respect to the ribitol internal standard. TMEV (<http://www.tm4.org/mev.html>) was used for all statistical analyses. Univariate analysis by permutation (one way-ANOVA) was used to select the significant metabolites. For glutathione measurements that are not possible using GC–MS, enzymatic assays were performed according to Noctor and Foyer (1998).

Quantitative RT-PCR for sulfate transporter mRNA quantification

To analyze the transcriptional levels of sulfate transporters in roots of Col and *sid2*, the seeds were sown on vertical plates containing 2 mM SO_4^{2-} (control, Ctrl) and 8.5 μM SO_4^{2-} (low sulfur, low-S), respectively, according to the compositions described in the Table S5. After 15 days, the roots of Col and *sid2* were harvested, and frozen immediately in liquid nitrogen. The harvested roots were stored at -80°C for further study. The total RNA was extracted from the roots using Trizol reagent (Ambion) according to the user's instruction. The trace genomic DNA was digested using DNase I RNase-free kit (EN0521, ThermoFisher Scientific) with RNase inhibitor (E00382, ThermoFisher Scientific). Then the first-strand cDNA was synthesized with M-MuLV Reverse Transcriptase kit (EP0352, ThermoFisher Scientific) according user's instruction. The qRT-PCR was performed on a CFX 96 thermocycler (Biorad) with specific primers (Table S6) according to Di Bernardino et al. (2018). The qRT-PCR was conducted in triplicate together with three biological replicates. Three genes (*UBC21*, *ACTIN 2* and *EF1 α*) were used as internal reference genes. Expression levels of genes were normalized to the geometrical mean of the three reference genes (*UBC21*, *ACTIN 2* and *EF1 α*), and relative expression levels were calculated according to the expression level compared to Col under Ctrl condition.

Bioinformatic analysis

All statistical analyses were performed using the R software (<https://www.R-project.org/>). Proteomic (XIC values) data were analyzed using Student's *t*-test and comparing Col and *sid2* genotypes in each growth conditions. The *P*-value was adjusted in R software by FDR correction (Benjamini & Hochberg, 1995). FDR lower than 0.05 and FC above (or lower) than 1.2 (or -1.2) were applied as cutoff. For transcriptome analyses, raw data (the CEL files) were normalized globally and expression levels were calculated in R software (<https://www.R-project.org/>) with limma package. The *P*-value was adjusted in R software by FDR correction (Benjamini & Hochberg, 1995). $\text{Log}_2(\text{FC})$ above (or lower) than 1 (or -1) and adjusted *P*-value lower than 0.05 were used as cutoff to select significant genes. The annotations of Affymetrix probe sets were obtained from TAIR (<https://www.arabidopsis.org/index.jsp>). Functional information and cellular location for each proteins

(or genes) were analyzed using VirtualPlant 1.3 (<http://virtualplant.bio.nyu.edu/cgi-bin/vpweb/>), MapMan (<https://mapman.gabipd.org/>) software and SUBA4 (<http://suba.live/>). GO and KEGG analyses were conducted using VirtualPlant 1.3, the *P*-value was adjusted by FDR correction (Benjamini & Hochberg, 1995). GO and KEGG terms with *P*-value (with FDR correction) lower than 0.05 were considered as statistically significant terms. Gene set enrichment analysis (GSEA) was conducted in R software with clusterProfiler package (Wu et al., 2021).

Statistical analyses

For chlorophyll related data, the data were checked for normality before the statistical analyses. Two-way ANOVA was preformed considering genotype and nutrition status as two factors. The differences between means were considered statistically significant, when *P*-values of ANOVA *F*-test were lower than 0.05. All the statistical analyses were conducted with Statgraphics (STN, St Louis, MO, USA). For other parameters, Student's *t*-test was conducted by comparing Col and *sid2* genotypes in each growth conditions.

ACKNOWLEDGMENT

Authors thank the proteomic platform PAPSSO (INRA, Le Moulon, France), the PLATIN plateforme of University of Normadie (Caen, France) and the "Plateforme Biopuces et Séquençage" of IGBMC (Strasbourg, France) for proteomic, isotope and transcriptomic analyses, respectively. Thanks to Philippe Maréchal for taking care of plants. Thanks to Dr. Jean-Luc Cacas for discussion about lipids. And to Prof. Alia Dellagi for discussion about SA and *npr1* relationships. This work has benefited from the support of IJPB's Plant Observatory technological platforms.

AUTHOR CONTRIBUTIONS

MH and TB performed the proteomic experiments under the supervision of MZ. JL and MH contributed to statistical analyses. JL performed the bioinformatic analyses and experiments related to sulfate transporters. J-CA performed S and ^{34}S measurements. GC performed metabolome analyses and FT the lipidomic analyses. CM-D supervised the entire work, interpreted results and wrote the manuscript.

FUNDING INFORMATION

This work was supported the ANR-12-ADAPT-0010-0. The LabEx Saclay Plant Sciences-SPS (ANR-10-LABX-0040-SPS) provided support for IJPB. J.L. was supported by AgreenSkills international program for mobility with the support of the AgreenSkills+ fellowship program which has received funding from the EU's Seventh Framework Program under agreement N° FRP7-609398 (AgreenSkill+ contract). M.H. was supported by ANR-12-ADAPT-0010-0.

SUPPORTING INFORMATION

Additional Supporting Information may be found in the online version of this article.

Figure S1. Phenotype of *sid2* depending on N and S conditions.

Figure S2. Chlorophyll concentration of *sid2* is lower than in WT while NahG-OE presents higher anthocyanins under low-S.

Figure S3. GO term enrichment analysis of the transcriptome using GSEA enrichment plot and ORA using VirtualPlant 1.3.

Figure S4. Significant changes in the abundance of the translation related proteins in *sid2* under low-S.

Dataset S1. Transcriptome of *sid2* vs. WT under low sulfate conditions.

Dataset S2. Significant protein changes under low-S compared to control conditions, in *sid2* and in WT.

Dataset S3. Significant protein changes in *sid2* under low-S and control conditions.

Dataset S4. Metabolome GC-MS analyses: raw data.

Table S1. GO terms associated to the proteins significantly differentially accumulated in low sulfate (Low-S) compared to control (Ctrl) condition in both wild type and *sid2*.

Table S2. GO terms associated to the proteins significantly differentially accumulated in *sid2* vs. WT under low sulfate (Low-S).

Table S3. Significant changes in the protein levels of sulfur-related proteins in *sid2* under low-S condition.

Table S4. Nutritive stock solutions for plant growth on sand.

Table S5. Composition of mediums used for vertical plates.

Table S6. Primers used in this study.

REFERENCES

- Abdallah, M., Dubouset, L., Meuriot, F., Etienne, P., Avice, J.C. & Oury, A. (2010) Effect of mineral sulphur availability on nitrogen and sulphur uptake and remobilization during the vegetative growth of Brassica napus L. *Journal of Experimental Botany*, **61**, 2635–2646.
- Abreu, M.E. & Munné-Bosch, S. (2009) Salicylic acid deficiency in NahG transgenic lines and *sid2* mutants increases seed yield in the annual plant Arabidopsis thaliana. *Journal of Experimental Botany*, **60**, 1261–1271.
- Benjamini, Y. & Hochberg, Y. (1995) Controlling the false discovery rate: a practical and powerful approach to multiple testing. *Journal of the Royal Statistical Society, Series B*, **57**, 289–300.
- Clément G, Moison M, Soulay F, Reisdorf-Cren M, Masclaux-Daubresse C. 2018. Metabolomics of laminae and midvein during leaf senescence and source-sink metabolite management in Brassica napus L. leaves. *J. Exp. Bot.* **69**, 891–903.
- Dempsey, D.A. & Klessig, D.F. (2017) How does the multifaceted plant hormone salicylic acid combat disease in plants and are similar mechanisms utilized in humans? *BMC Biology*, **15**, 23.
- Di Bernardino J, Marmagne A, Berger A, Yoshimoto K, Cuffe G, Chardon F, Masclaux-Daubresse C, Reisdorf-Cren M. 2018. Autophagy Controls Resource Allocations and Protein Storage Accumulation in Arabidopsis Seeds. *J. Exp. Bot.* **69**, 1403–1414.
- Dibble, C.C., Barritt, S.A., Perry, G.E., Lien, E.C., Geck, R.C., DuBois-Coyne, S.E. et al. (2022) PI3K drives the de novo synthesis of coenzyme a from vitamin B5. *Nature*, **608**, 192–198.
- Dietzen, C., Koprivova, A., Whitcomb, S.J., Langen, G., Jobe, T.O., Hoefgen, R. et al. (2020) The transcription factor EIL1 participates in the regulation of sulfur-deficiency response. *Plant Physiology*, **184**, 2120–2136.
- Dubouset, L., Abdallah, M., Desfeux, A.S., Etienne, P., Meuriot, F., Hawkesford, M.J. et al. (2009) Remobilization of leaf S compounds and senescence in response to restricted sulphate supply during the vegetative stage of oilseed rape are affected by mineral N availability. *Journal of Experimental Botany*, **60**, 3239–3253.
- Dubouset, L., Etienne, P. & Avice, J. (2010) Is the remobilization of S and N reserves for seed filling of winter oilseed rape modulated by Sulphate restrictions occurring at different growth stages? *Journal of Experimental Botany*, **61**, 4313–4324.
- Edgar, R., Domrachev, M. & Lash, A.E. (2002) Gene expression omnibus: NCBI gene expression and hybridization array data repository. *Nucleic Acids Res.*, **30**, pp.207–210.
- Faize, L. & Faize, M. (2018) Functional analogues of salicylic acid and their use in crop protection. *Agronomy-Basel*, **8**(1), 5.
- Ghazijahani, N., Hadavi, E. & Jeong, B.R. (2014) Foliar sprays of citric acid and salicylic acid alter the pattern of root acquisition of some minerals in sweet basil (*Ocimum basilicum* L.). *Frontiers in Plant Science*, **5**, 573.
- Gironde, A., Dubouset, L., Trouverie, J., Etienne, P. & Avice, J.C. (2014) The impact of sulfate restriction on seed yield and quality of winter oilseed rape depends on the ability to remobilize sulfate from vegetative tissues to reproductive organs. *Frontiers in Plant Science*, **5**, 695.
- Guo, P.R., Li, Z.H., Huang, P.X., Li, B.S., Fang, S., Chu, J.F. et al. (2017) A tripartite amplification loop involving the transcription factor WRKY75, salicylic acid, and reactive oxygen species accelerates leaf senescence. *Plant Cell*, **29**, 2854–2870.
- Hao, J.H., Wang, X.L., Dong, C.J., Zhang, Z.G. & Shang, Q.M. (2011) Salicylic acid induces stomatal closure by modulating endogenous hormone levels in cucumber cotyledons. *Russian Journal of Plant Physiology*, **58**, 906–913.
- Havé, M., Balliau, T., Cottyn-Boitte, B., Derond, E., Cuffe, G., Soulay, F. et al. (2018) Increase of proteasome and papain-like cysteine protease activities in autophagy mutants: backup compensatory effect or pro cell-death effect? *Journal of Experimental Botany*, **69**, 1369–1385.
- Havé, M., Luo, J., Tellier, F., Balliau, T., Cuffe, G., Chardon, F. et al. (2019) Proteomic and lipidomic analyses of the Arabidopsis atg5 autophagy mutant reveal major changes in ER and peroxisome metabolisms and in lipid composition. *New Phytologist*, **223**, 1461–1477.
- Havé, M., Marmagne, A., Chardon, F. & Masclaux-Daubresse, C. (2017) Nitrogen remobilization during leaf senescence: lessons from Arabidopsis to crops. *Journal of Experimental Botany*, **68**, 2513–2529.
- Khokon, M.A.R., Okuma, E., Hossain, M.A., Munemasa, S., Uraji, M., Nakamura, Y. et al. (2011) Involvement of extracellular oxidative burst in salicylic acid-induced stomatal closure in Arabidopsis. *Plant, Cell & Environment*, **34**, 434–443.
- Kim, J., Kim, J.H., Lyu, J.I., Woo, H.R. & Lim, P.O. (2018) New insights into the regulation of leaf senescence in Arabidopsis. *Journal of Experimental Botany*, **69**, 787–799.
- Lornac, A., Havé, M., Chardon, F., Soulay, F., Clément, G., Avice, J.C. et al. (2020) Autophagy controls sulphur metabolism in the rosette leaves of Arabidopsis and facilitates S remobilization to the seeds. *Cells*, **9**, 332.
- Luo, J., Havé, M., Clément, G., Tellier, F., Balliau, T., Launay-Avon, A. et al. (2020) Integrating multiple omics to identify common and specific molecular changes occurring in Arabidopsis under chronic nitrate and sulfate limitations. *Journal of Experimental Botany*, **71**, 6471–6490.
- Mauch, F., Mauch-Mani, B., Gaille, C., Kull, B., Haas, D. & Reimmann, C. (2001) Manipulation of salicylate content in Arabidopsis thaliana by the expression of an engineered bacterial salicylate synthase. *Plant Journal*, **25**, 67–77.
- McNeill, A.M., Eriksen, J., Bergstrom, L., Smith, K.A., Marstorp, H., Kirchmann, H. et al. (2005) Nitrogen and sulphur management: challenges for organic sources in temperate agricultural systems. *Soil Use and Management*, **21**, 82–93.
- Morris, K., MacKerness, S.A., Page, T., John, C.F., Murphy, A.M., Carr, J.P. et al. (2000) Salicylic acid has a role in regulating gene expression during leaf senescence. *The Plant Journal*, **23**, 677–685.
- Nazar, R., Iqbal, N., Syeed, S. & Khan, N.A. (2011) Salicylic acid alleviates decreases in photosynthesis under salt stress by enhancing nitrogen and sulfur assimilation and antioxidant metabolism differentially in two mungbean cultivars. *Journal of Plant Physiology*, **168**, 807–815.
- Noctor G, Foyer CH. 1998. Simultaneous measurement of foliar glutathione, gamma-glutamylcysteine, and amino acids by high-performance liquid chromatography: Comparison with two other assay methods for glutathione. *Anal. Biochem.* **264**, 98–110.
- Peng, Y., Yang, J., Li, X. & Zhang, Y. (2021) Salicylic acid: biosynthesis and signaling. *Annual Reviews*, **72**, 761–791.
- Pokotylo, I., Kravets, V. & Ruelland, E. (2019) Salicylic acid binding proteins (SABPs): the hidden forefront of salicylic acid signalling. *International Journal of Molecular Sciences*, **20**(18), 4377.
- Rouached, H., Wirtz, M., Alary, R., Hell, R., Bulak Arpat, A., Davidian, J.C. et al. (2008) Differential regulation of the expression of two high-affinity sulfate transporters Sultr 1;1 and Sultr 1;2 in Arabidopsis. *Plant Physiology*, **147**, 897–911.
- Sasek, V., Janda, M., Delage, E., Puyaubert, J., Guivarc'h, A., Maseda, E.L. et al. (2014) Constitutive salicylic acid accumulation in pi4kll beta 1 beta

- 2 Arabidopsis plants stunts rosette but not root growth. *New Phytologist*, **203**, 805–816.
- Shannon, P., Markiel, A., Ozier, O., Baliga, N.S., Wang, J.T., Ramage, D. et al.** (2003) Cytoscape: a software environment for integrated models of biomolecular interaction networks. *Genome Research*, **13**, 2498–2504.
- Shen, C., Yang, Y., Liu, K., Zhang, L., Guo, H., Sun, T. et al.** (2016) Involvement of endogenous salicylic acid in iron-deficiency responses in Arabidopsis. *Journal of Experimental Botany*, **67**, 4179–4193.
- Sirko, A., Wawrzynska, A., Rodriguez, M.C. & Sektas, P.** (2015) The family of LSU-like proteins. *Frontiers in Plant Science*, **5**, 774.
- Sorin, E., Etienne, P., Maillard, A., Zamarreno, A.M., Garcia-Mina, J.M., Arkoun, M. et al.** (2015) Effect of sulphur deprivation on osmotic potential components and nitrogen metabolism in oilseed rape leaves: identification of a new early indicator. *Journal of Experimental Botany*, **66**, 6175–6189.
- Speiser, A., Silbermann, M., Dong, Y.H., Haberland, S., Uslu, V.V., Wang, S.S. et al.** (2018) Sulfur partitioning between glutathione and protein synthesis determines plant growth. *Plant Physiology*, **177**, 927–937.
- Szklarczyk, D., Gable, A.L., Nastou, K.C., Lyon, D., Kirsch, R., Pyysalo, S. et al.** (2021) The STRING database in 2021: customizable protein–protein networks, and functional characterization of user-uploaded gene/measurements sets. *Nucleic Acids Research*, **49**, D605–D612.
- Thaler, J.S., Humphrey, P.T. & Whiteman, N.K.** (2012) Evolution of jasmonate and salicylate signal crosstalk. *Trends in Plant Science*, **17**, 260–270.
- Velasco, V.M.E., Mansbridge, J., Bremner, S., Carruthers, K., Summers, P.S., Sung, W.W.L. et al.** (2016) Acclimation of the crucifer *Eutrema salicagineum* to phosphate limitation is associated with constitutively high expression of phosphate-starvation genes. *Plant, Cell & Environment*, **39**, 1818–1834.
- Vergnes, S., Ladouce, N., Fournier, S., Ferhout, H., Attia, F. & Dumas, B.** (2014) Foliar treatments with *Gaultheria procumbens* essential oil induce defense responses and resistance against a fungal pathogen in Arabidopsis. *Frontiers in Plant Science*, **5**, 477.
- Weigel, R.R., Pfitzner, U.M. & Gatz, C.** (2005) Interaction of NIMIN1 with NPR1 modulates PR gene expression in Arabidopsis. *Plant Cell*, **17**, 1279–1291.
- Wildermuth, M.C., Dewdney, J., Wu, G. & Ausubel, F.M.** (2001) Isochorismate synthase is required to synthesize salicylic acid for plant defence. *Nature*, **414**, 562–565.
- Wu, J., Zhu, W. & Zhao, Q.** (2022) Salicylic acid biosynthesis is not from phenylalanine in Arabidopsis. *Journal of Integrative Plant Biology*, **65**, 881–887. Available from: <https://doi.org/10.1111/jipb.13410>
- Wu, T., Hu, E., Xu, S., Chen, M., Guo, P., Dai, Z. et al.** (2021) clusterProfiler 4.0: a universal enrichment tool for interpreting omics data. *The Innovations*, **2**(3), 100141.
- You, I.S., Ghosal, D. & Gunsalus, I.C.** (1991) Nucleotide-sequence analysis of the *Pseudomonas-putida* PPG7 salicylate hydroxylase gene (NAHG) and its 3'-flanking region. *Biochemistry*, **30**, 1635–1641.